Transportation Research Part C 86 (2018) 441–452

Contents lists available at ScienceDirect

Transportation Research Part C

journal homepage: www.elsevier.com/locate/trc

Microscopic simulation-based validation of a per-lane traffic state estimation scheme for highways with connected vehicles

Sofia Papadopoulou[a,*], Claudio Roncoli[b], Nikolaos Bekiaris-Liberis[a], Ioannis Papamichail[a], Markos Papageorgiou[a]

[a] Dynamic Systems and Simulation Laboratory, School of Production Engineering and Management, Technical University of Crete, Chania 73100 Greece

[b] Department of Built Environment, School of Engineering, Aalto University, Espoo 02150 Finland

ARTICLE INFO

Keywords:
Traffic state estimation
Connected vehicles
Kalman filter
Microscopic simulation testing

ABSTRACT

This study presents a thorough microscopic simulation investigation of a recently developed model-based approach for per-lane density estimation, as well as on-ramp and off-ramp flow estimation, for highways in the presence of connected vehicles. The estimation methodology is mainly based on the assumption that a certain percentage of vehicles is equipped with Vehicle Automation and Communication Systems (VACS), which provide the necessary measurements used by the estimator, namely vehicle speed and position measurements. In addition, a minimum number of conventional flow detectors is needed. In the investigation, a calibrated and validated, with real data, microscopic multi-lane model is employed, which concerns a stretch of motorway A20 from Rotterdam to Gouda in the Netherlands. It is demonstrated that the proposed methodology provides satisfactory estimation performance even for low penetration rates of connected vehicles, while it is also shown that the method is little sensitive to the parameters (two in total) of the model utilized by the estimator.

1. Introduction

Most cities around the world experience ever-growing traffic congestion in urban areas and motorway networks. Congestion may be mitigated by optimizing the performance of the traffic infrastructure through traffic management and operational strategies. Real-time traffic information is a prerequisite for traffic operations, such as freeway ramp metering control, dynamic route guidance, incident detection, and variable message sign operations. In recent years, VACS are all the more receiving considerable attention since they may create new principles in traffic management, as they are capable of communicating real-time information and execute novel control tasks (Papageorgiou et al., 2015). Considering that density distribution may be highly heterogeneous among the different lanes of a highway, real-time lane assignment strategies may have significant advantages in traffic management. Lane policies and lane advice may be achieved if real-time traffic state information per lane is available (Roncoli et al., 2016b, 2017).

Recently, research on exploiting the innovative characteristics of VACS as a source of traffic data in traffic state estimation has drawn some attention, primarily due to the low cost, wide coverage and high accuracy of the extracted data. In this work, we consider that connected vehicles are vehicles capable of reporting information (i.e., position and speed) to an infrastructure-based system, which may be achieved via different technologies and communication paradigms. A basic scenario may simply consist of vehicles

* Corresponding author.
E-mail addresses: spapadopoulou@isc.tuc.gr (S. Papadopoulou), claudio.roncoli@aalto.fi (C. Roncoli), nikos.bekiaris@dssl.tuc.gr (N. Bekiaris-Liberis), ipapa@dssl.tuc.gr (I. Papamichail), markos@dssl.tuc.gr (M. Papageorgiou).

https://doi.org/10.1016/j.trc.2017.11.012
Received 25 April 2017; Received in revised form 28 September 2017; Accepted 11 November 2017

equipped with a GPS (Global Positioning System) and a system for mobile communication. However, more complex scenarios, for example, scenarios that incorporate communication among vehicles or between vehicles and roadside units, are also possible. Connected vehicles use localization technologies that can provide these data such as Dedicated Short-Range Communications (DSRC), as well as Global Positioning Systems (GPS), cellular and Bluetooth. Data stemming from connected vehicles may contain a variety of essential dynamic transportation information, while the most commonly used are vehicle position (longitude, latitude, and altitude) and vehicle speed. Global Positioning System (GPS) receivers are stated as the most popular communication system because they are low-cost, efficient and are already commonplace in many vehicles, in use for navigation. GPS systems have stated accuracy ranging from 5 to 15 m in geographical positioning Zito et al. (1995), Turksma (2000), and Liu et al. (2006). But most modern methods adopt a hybrid positioning system, combining differential GPS (DGPS) with map-matching and dead-reckoning, which improved vehicle position data up to 1–5 m accuracy Waterson and Box (2012), sufficient for lane-based applications. Speed measurements are mostly reported to be quite accurate with a precision error lower than 1 km/h Chalko (2007) and Zito et al. (1995), while some studies claim a tendency of underestimation in speed measurements and a reported error around 5 km/h Zhao et al. (2014).

Traffic state estimation utilizing floating car data has been investigated in numerous studies, such as, for example, Work et al. (2008), Fabritiis et al. (2008), Herrera et al. (2010), Herrera and Bayen (2010), Rahmani et al. (2010), Qiu et al. (2010), Schreiter et al. (2010), Treiber et al. (2011), Yuan et al. (2012), van Hinsbergen et al. (2012), Deng et al. (2013), Anand et al. (2014), Piccoli et al. (2015), Seo et al. (2015), Seo and Kusakabe (2015), Rempe et al. (2016), Wang et al. (2016), Wright and Horowitz (2016), Bekiaris-Liberis et al. (2016), Roncoli et al. (2016a), Seo et al. (2017), and Fountoulakis et al. (2017). While multi-lane traffic flow modeling has been the subject of several works (Laval and Daganzo, 2006; Roncoli et al., 2015; Carey et al., 2015; Du et al., 2016), the existing studies that deal with lane-based traffic state estimation are rare in the traffic literature, while they mainly assume data obtained from conventional detectors (Chang and Gazis, 1975; Coifman, 2003; Singh and Li, 2012; Yılan, 2016) with the exception of Zhou and Mirchandani (2015).

This paper presents several novelties with respect to our previous works and to other approaches published in the last decade. Existing works in literature dealing with the problem of lane-based traffic state estimation mainly assume data obtained from conventional detectors. Thus, the available measurement information as well as the measurement configurations employed in the present paper are different from those required in almost all other lane-based estimation approaches. Previous works (Bekiaris-Liberis et al., 2016; Roncoli et al., 2016a; Fountoulakis et al., 2017) employed connected vehicle data to estimate only cross-lane densities and on-ramp flows. In contrast, in the present paper, we implement a different model and we use a different measurement configuration to enable per-lane density estimation. Nevertheless, the distinguishing feature of our previous works, namely the lack of the need for any empirical modeling approach, such as fundamental diagrams, that would call for tedious calibration procedures, is present here as well.

The main contribution of this paper is the thorough evaluation of a per-lane density and ramp flow estimation methodology via microscopic simulation, including different penetration rates of connected vehicles. The estimation scheme uses a data-driven macroscopic model for per-lane traffic density and employs real-time measurements obtained from connected vehicles, namely vehicles which transmit information about their position and speed. A minimum number of spot flow measurements from detectors is also needed to guarantee the observability property of the underlying model, see Bekiaris-Liberis et al. (2017) for details. Density estimation is performed via the employment of a Kalman filter. The performance of the estimation scheme is examined under various penetration rates of connected vehicles, using data retrieved from a microscopic multi-lane model, which has been calibrated and validated by Perraki et al. (2017) with real data from a stretch of motorway A20 from Rotterdam to Gouda in The Netherlands. The case-study highway stretch includes several on-ramps, off-ramps, and a lane-drop, while the employed simulation scenario is characterized by both congested and free-flow traffic conditions. Thus, the effectiveness of the proposed methodology is examined in carefully designed experiments for a real highway stretch with real demand scenarios. It is worth mentioning that, in the investigation, simple algorithms are employed in case of inconsistencies in the probe vehicle data (such as, for instance, in case there are temporarily no measurements available from connected vehicles). The performance of the tested estimation scheme is shown to be satisfactory even for low penetration rates. Finally, it is demonstrated that estimation performance is little sensitive to the choice of the model parameters (two in total).

The remainder of the paper is organized as follows. The model for the per-lane density dynamics and the proposed estimation scheme are presented in Section 2. The description of the microscopic simulation configuration as well as the highway network under study and the traffic conditions are presented in Section 3, which includes also the details of the computation of the data employed by the estimator. Subsequently, the results of the estimation and a sensitivity analysis of the estimation performance with regard to the model parameters are presented in Section 4. Finally, in Section 5 the main findings of this study are summarized.

2. Per-lane traffic state estimation using a data-driven model

2.1. General set-up

We consider a highway stretch consisting of M lanes, indexed by $j = 1,...,M$, subdivided into N segments, indexed by $i = 1,...,N$. We define a cell (i,j) to be the highway part that corresponds to lane j of segment i. The length of each segment is denoted by $\Delta_i, i = 1,...,N$.

The following variables are extensively used in the paper:

- Space mean speed $\left[\frac{\text{km}}{\text{h}}\right]$ of vehicles in cell (i,j), denoted by $v_{i,j}$, for $i = 1,...,N$ and $j = 1,...,M$.
- Total traffic density $\left[\frac{\text{veh}}{\text{km}}\right]$ at cell (i,j), denoted by $\rho_{i,j}$, for $i = 1,...,N$ and $j = 1,...,M$.
- Total longitudinal inflow $\left[\frac{\text{veh}}{\text{h}}\right]$ of cell $(i+1,j)$, denoted by $q_{i,j}$, for $i = 0,...,N-1$ and $j = 1,...,M$.
- Total on-ramp flow $\left[\frac{\text{veh}}{\text{h}}\right]$ entering at cell (i,j), denoted by $r_{i,j}$, for $i = 1,...,N$ and $j = 1,...,M$.
- Total off-ramp flow $\left[\frac{\text{veh}}{\text{h}}\right]$ exiting from cell (i,j), denoted by $s_{i,j}$, for $i = 1,...,N$ and $j = 1,...,M$.
- Total lateral flow $\left[\frac{\text{veh}}{\text{h}}\right]$ at segment i that enters lane j_2 from lane j_1, denoted by $L_{i,j_1\to j_2}$, for $i = 1,...,N, j_1 = 1,...,M$, and $j_2 = j_1 \pm 1$.

Note that, the attribute "total" refers to the total population of both connected and conventional vehicles.

2.2. Available information from connected vehicle reports

The data-driven model presented in the next subsection, requires the availability of the following measurements:

- Space mean speed of connected vehicles at cell (i,j), denoted by $v^{c}_{i,j}$, for $i = 1,...,N$ and $j = 1,...,M$.
- Density of connected vehicles at cell (i,j), denoted by $\rho^{c}_{i,j}$, for $i = 1,...,N$ and $j = 1,...,M$.
- Lateral flow of connected vehicles at segment i that enters lane j_2 from lane j_1, denoted by $L^{c}_{i,j_1\to j_2}$, for $i = 1,...,N, j_1 = 1,...,M$, and $j_2 = j_1 \pm 1$.

Average speeds, densities, and lateral flows of connected vehicles may be readily obtained from position and speed reports.

2.3. Model description for the density and ramp flow dynamics

The conservation equation yields the following model for the density dynamics in each cell (i,j)

$$\rho_{i,j}(k+1) = \rho_{i,j}(k) + \frac{T}{\Delta_i}\left(q_{i-1,j}(k) - q_{i,j}(k) + L_{i,j-1\to j}(k) + L_{i,j+1\to j}(k) - L_{i,j\to j-1}(k) - L_{i,j\to j+1}(k) + r_{i,j}(k) - s_{i,j}(k)\right), \tag{1}$$

where T is the time discretization step. For convenience, we assume $r_{i,j} \equiv s_{i,j} \equiv 0$, $\forall\, i$ and $1 \le j \le M-1$, where M denotes the rightmost lane (assuming right-hand traffic); we have $L_{i,j_1\to j_2} \equiv 0$ if either j_1 or j_2 equals zero or $M+1$. Moreover, in case there is a lane-drop at cell (i,j), then we define $q_{i,j}(k) \equiv 0$. We note that the per-lane inflows at the highway entry, namely, $q_{0,j}$, $j = 1,...,M$, are treated as measured inputs to system (1).

The following relation is employed for total flows (Fig. 1)

$$q_{i,j}(k) = v_{i,j}(k)\rho_{i,j}(k) + p_{i,j-1\to j}L_{i,j-1\to j}(k) + p_{i,j+1\to j}L_{i,j+1\to j}(k) + \overline{p}_{i,j}r_{i,j}(k), \tag{2}$$

for $i = 1,...,N, j = 1,...,M$, where $p_{i,j_1\to j_2}, \overline{p}_{i,j} \in [0,1]$,$\forall\, (i,j), j_1 = 1,...,M$, and $j_2 = j_1 \pm 1$, indicate the percentages of "diagonal" lateral movements, including lateral flows from an on-ramp acceleration lane, for each specific cell. While the first term in (2) is well-known (see, e.g., Papageorgiou and Messmer, 1999), the motivation for the rest of the terms may be less obvious. Their choice is guided from the fact that, at locations featuring strong lateral flows (e.g., at cells where an on-ramp is located or at segments that feature lane-drops), a significant amount of the lateral flow may appear close to the cell end (e.g., in the former case, at the acceleration lane end). As a result, the flow modeling may be more accurately described considering that a percentage of lateral or on-ramp flows actually acts as additional exiting longitudinal flow. This formulation is also employed in other works, e.g., Laval and Daganzo (2006).

For the lateral flows, we employ the following relation

$$L_{i,j_1\to j_2}(k) = \frac{L^{c}_{i,j_1\to j_2}(k)}{\rho^{c}_{i,j_1}(k)}\rho_{i,j_1}(k), \tag{3}$$

for $i = 1,...,N, j_1 = 1,...,M$, and $j_2 = j_1 \pm 1$. Eq. (3) is based on the reasonable assumption that the average behavior of the population of

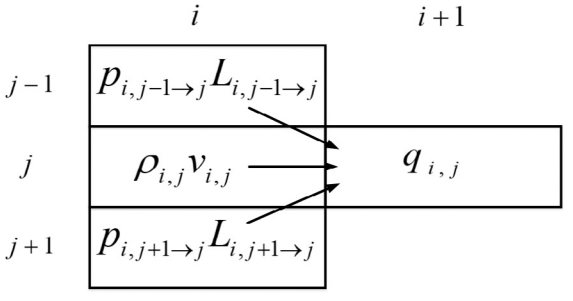

Fig. 1. Model of the exiting longitudinal flow from cell (i,j) as described in (2).

connected vehicles in a given cell, with respect to lateral movements, is representative for the total vehicle population in that cell. This assumption relies on the fact that, since we consider as connected vehicle any vehicle that incorporates a communication system and thus, is capable of providing traffic information to an infrastructure-based system, there is no reason for connected vehicles to feature a systematically different behavior than manual vehicles. Moreover, also in case connected vehicles feature some degree of automation, we expect a proper operation of our estimations scheme. More specifically, in case there is no strict infrastructure-based need for lane changing, lane-changing flows are very low, hence we could even utterly ignore lane changing and still obtain reasonable estimation results. On the other hand, in case there is a strict infrastructure-based need for lane changing (such as, for example, near ramps or a lane drop), strong lateral flows occur and need to be measured. However, in such cases, automated vehicles, like manually driven vehicles, have not much of other choice than to change lane. These lane-changes may happen slightly earlier or later than manual vehicles, but roughly in proportions that are similar to what manual vehicles also need to perform, and this is in fact what (3) reflects.

This assumption allows one to quantify the total lateral movements from a cell using (3), namely, by scaling the lateral movements of connected vehicles with the *inverse* of the percentage of connected vehicles in that cell.

Plugging (2) and (3) into (1), we get for all (i,j)

$$\begin{aligned}\rho_{i,j}(k+1) = &\left(1-\frac{T}{\Delta_i}v_{i,j}(k)-\frac{T}{\Delta_i}\frac{L^{c}_{i,j\to j-1}(k)}{\rho^{c}_{i,j}(k)}-\frac{T}{\Delta_i}\frac{L^{c}_{i,j\to j+1}(k)}{\rho^{c}_{i,j}(k)}\right)\rho_{i,j}(k)+\frac{T}{\Delta_i}v_{i-1,j}(k)\times\rho_{i-1,j}(k)\\ &+\frac{T}{\Delta_i}\left((1-p_{i,j-1\to j})\frac{L^{c}_{i,j-1\to j}(k)}{\rho^{c}_{i,j-1}(k)}\rho_{i,j-1}(k)+(1-p_{i,j+1\to j})\times\frac{L^{c}_{i,j+1\to j}(k)}{\rho^{c}_{i,j+1}(k)}\rho_{i,j+1}(k)\right)\\ &+\frac{T}{\Delta_i}\left(p_{i-1,j-1\to j}\frac{L^{c}_{i-1,j-1\to j}(k)}{\rho^{c}_{i-1,j-1}(k)}\rho_{i-1,j-1}(k)+p_{i-1,j+1\to j}\frac{L^{c}_{i-1,j+1\to j}(k)}{\rho^{c}_{i-1,j+1}(k)}\rho_{i-1,j+1}(k)\right)+(1-\overline{p}_{i,j})\frac{T}{\Delta_i}r_{i,j}(k)\\ &+\frac{T}{\Delta_i}(\overline{p}_{i-1,j}r_{i-1,j}(k)-s_{i,j}(k)).\end{aligned} \tag{4}$$

We adopt, as usual in absence of a descriptive dynamic model (see Wang and Papageorgiou, 2005), a random walk to describe the dynamics of on-ramp and off-ramp flows. The deterministic parts of such models read

$$r_{i,M}(k+1) = r_{i,M}(k) \tag{5}$$

$$s_{i,M}(k+1) = s_{i,M}(k). \tag{6}$$

We write next compactly the overall system (4)–(6). For this, we define first the state vector x as follows

$$x = (\rho_{1,1},\dots,\rho_{N,1},\dots,\rho_{1,M}\dots,\rho_{N,M},r_{1,M},\dots,r_{N,M},s_{1,M},\dots,s_{N,M})^{\mathrm{T}}. \tag{7}$$

The average speed of connected vehicles is representative of the average cell speed, as motivated in Bekiaris-Liberis et al. (2016) and justified with real data and in microscopic simulation in Roncoli et al. (2016a) and Fountoulakis et al. (2017), respectively, even for connected-vehicle penetrations as low as 2%. Thus, the unmeasured cell speeds $v_{i,j}$ may be replaced by the corresponding measured speeds $v^{c}_{i,j}$; and, using (7), we re-write (4)–(6) in a compact form as

$$x(k+1) = A(v^{c}(k),L^{c}(k),\rho^{c}(k))x(k)+Bu(k), \tag{8}$$

where v^{c}, L^{c}, and ρ^{c} denote vectors that incorporate all average cell speeds of connected vehicles $v^{c}_{i,j}$, lateral flows of connected vehicles $L^{c}_{i,j_1\to j_2}$, and densities of connected vehicles $\rho^{c}_{i,j}$, respectively; while u denotes the vector of inflows at the highway entrance, namely $u = (q_{0,1},\dots,q_{0,M})^{\mathrm{T}}$, $A\in\mathbb{R}^{(N\times M+2N)\times(N\times M+2N)}$, and $B\in\mathbb{R}^{(N\times M+2N)\times M}$.

Together with (8), we associate an output vector y, which holds all mainstream total flows that are measured by corresponding mainstream fixed detectors and, as follows from (2) and (3), is given by

$$y(k) = C(v^{c}(k),L^{c}(k),\rho^{c}(k))x(k), \tag{9}$$

where $C\in\mathbb{R}^{(M+l_r+l_s-1)\times(N\times M+2N)}$, with l_r and l_s being the number of on-ramps and off-ramps, respectively. The minimum number of rows of C equals $M+l_r+l_s-1$ in order for system (8), (9) to be observable (see Bekiaris-Liberis et al. (2016, 2017) for details). Note that we assume $2N$ ramp flows. In the case where there are less on-ramp or off-ramp flows, the dimensions of the matrices A,B, and C are reduced accordingly.

2.4. Per-lane total density and ramp flow estimation utilizing a Kalman filter

We employ a standard Kalman filter utilizing model (8), (9) for per lane total density estimation. Defining the vector $\hat{x}$ as the system state to be estimated,

$$\hat{x} = (\hat{\rho}_{1,1},\dots,\hat{\rho}_{N,1},\dots,\hat{\rho}_{1,M},\dots,\hat{\rho}_{N,M},\hat{r}_{1,M},\dots,\hat{r}_{N,M},\hat{s}_{1,M},\dots,\hat{s}_{N,M})^{\mathrm{T}}, \tag{10}$$

the filter equations are

$$\hat{x}(k+1) = A(v^{c}(k),L^{c}(k),\rho^{c}(k))\hat{x}(k)+Bu(k)+A(v^{c}(k),L^{c}(k),\rho^{c}(k))K(k)(z(k)-C(v^{c}(k),L^{c}(k),\rho^{c}(k))\hat{x}(k)) \tag{11}$$

$$K(k) = P(k)C(v^c(k),L^c(k),\rho^c(k))^{\mathrm{T}} \times (C(v^c(k),L^c(k),\rho^c(k))P(k)C(v^c(k),L^c(k),\rho^c(k))^{\mathrm{T}} + R)^{-1} \quad (12)$$

$$P(k+1) = A(v^c(k),L^c(k),\rho^c(k))(I - K(k)C(v^c(k),L^c(k),\rho^c(k))) \times P(k)A(v^c(k),L^c(k),\rho^c(k))^{\mathrm{T}} + Q, \quad (13)$$

where z is a noisy version of the measurement y defined in (9), $Q = Q^T \succ 0$ and $R = R^T \succ 0$ are tuning parameters which, in the ideal case in which there is additive, zero-mean Gaussian white noise in the state (8) and output (9) equations, represent the covariance matrices of the process and measurement noise, respectively. The initial conditions of the filter described by Eqs. (11)–(13) are

$$\hat{x}(k_0) = \mu \quad (14)$$

$$P(k_0) = H, \quad (15)$$

where μ and $H = H^T \succ 0$, represent, in the ideal case in which $x(k_0)$ is a Gaussian random variable, represent the mean and auto covariance matrix of $x(k_0)$, respectively.

3. Microscopic simulation set-up

The behavior of the proposed estimation scheme is examined and evaluated through microscopic simulation using AIMSUN (Transport Simulation Systems, 2014). Traffic measurements are extracted from a specific subset of the whole population of vehicles in the network that are considered to be connected. Vehicles entering the network are all of the same vehicle type, featuring a probabilistic distribution of movement behaviors, and are randomly marked as connected according to an assumed penetration rate, based on a uniform distribution.

3.1. Network and experimental configuration

The case-study network (see Fig. 2) is a stretch of motorway A20 from Rotterdam to Gouda, in the Netherlands. The multi-lane microscopic model employed in AIMSUN was designed and calibrated by Perraki et al. (2017) with real, lane-specific traffic data obtained from detectors (Schakel and Van Arem, 2014), thus providing a realistic ground truth scenario.

The considered highway stretch, shown in Fig. 2, constitutes a challenging test-bed for the proposed estimation scheme, as it incorporates a non-trivial combination of a lane-drop, on-ramps and off-ramps, which trigger a variety of corresponding lane-changing behaviors. The considered stretch is about 9.33 km in length, comprises 3 homo-directional lanes until 3.53 km, where there is a lane-drop. For the purpose of estimation, the stretch is space-discretised in $N = 21$ segments. Two on-ramps and two off-ramps are located at 3.08 km, 5.48 km and 4.17 km, 7.24 km, respectively.

The ground truth in our experiments, used to evaluate the performance of the developed estimation scheme, is represented by the total density in each cell and the total ramp flows. The cell densities $\rho_{i,j}$ are computed by counting the number of all vehicles that are present within cell (i,j) at a time instant kT, divided by the segment length Δ_i; whereas all ramp flows are computed by counting the number of vehicles that cross the corresponding location within the time interval $(kT,(k+1)T]$. However, since lane-based densities and ramp flows are very noisy, a moving average of the 6 latest available measurements is considered as ground truth. Average segment speeds $v_{i,j}$ that represent ground truth are computed by averaging arithmetically at time step kT the instant speeds of all vehicles present in a segment.

3.2. Employed scenario

The employed scenario utilizes available real demand measurements and replicates traffic conditions, whereby a strong congestion is created at 4 km at around 6:30 AM because of the increased flow entering from on-ramp Nieuwerkerk a/d IJssel. The congestion spills back, strengthens at the lane-drop at 3.6 km, and covers the stretch up to 1.2 km. From 7:00 AM until 7:30 AM, the congestion persists downstream of the lane-drop, while congestion upstream thereof dissolves. Fig. 3-(left column), illustrates the densities along each lane from 5:00 AM to 9:00 AM. This congestion pattern allows to test and evaluate the proposed estimator under varying traffic conditions, which include the formation and dissipation of a stretch-internal congestion, which is not visible at the stretch boundaries.

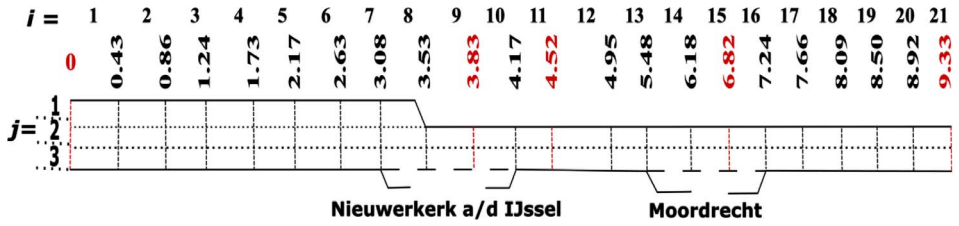

Fig. 2. Schematic representation of the case study network. Field detector positions are indicated as the distance (in km) from the network entrance. The detectors used by the estimator for obtaining flow measurements within the case study are colored in red. (For interpretation of the references to color in this figure legend, the reader is referred to the web version of this article.)

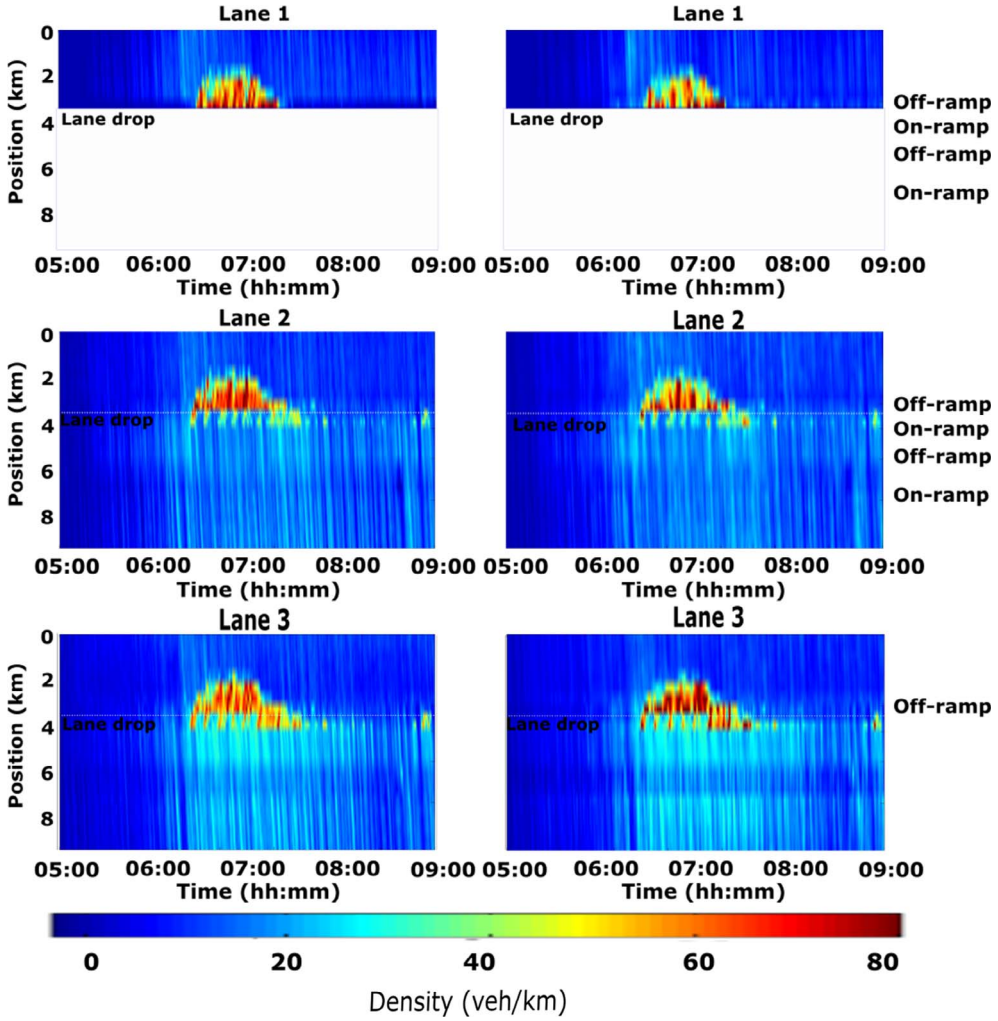

Fig. 3. Contour plot for the ground truth (left column) and estimated (right column) densities.

3.3. Computation of data employed by the estimator

Prior to the performance evaluation of the proposed estimation scheme, we detail the information provided to the estimator. The estimation performance depends critically on the quality of this information, thus we employ simple algorithms to ensure that this information is reliable and as representative as possible.

We consider a time discretization step $T = 10$ s. During a time interval $((k-1)T,kT]$, especially at light traffic and low penetrations rates, only few or even no connected vehicles may be present in a cell. Therefore, appropriate procedures must be applied to ensure that the estimation scheme will nevertheless be fed with appropriate real-time information.

To start with, speed reports from connected vehicles are collected every 2 s and are averaged arithmetically over every 10 s time period $((k-1)T,kT]$ to produce $v^{c}_{i,j}(k)$, denoted the average speed of connected vehicles at cell (i,j). This average speed corresponds to the space mean speed, since the connected vehicles are distributed within the respective cell; therefore, the average speed verifies (3). In cases where there are no connected vehicle reports available at cell (i,j) during a time interval $((k-1)T,kT]$, we set the missing value equal to the speed reported at the previous time step, i.e., we set $v^{c}_{i,j}(k) = v^{c}_{i,j}(k-1)$. However, at low penetration rates or light traffic, a cell may feature complete absence of connected vehicle reports, for more than one minute. For achieving better estimation results, especially for low penetration rates, we consider a larger time window over which we average the n past values of the average cell speeds from connected vehicle reports. In our experiments, we have tried different values for n. A complete absence of connected vehicle reports over 12 time intervals is very rare in our experiments, and thus, the moving average of speeds calculated with $n = 12$ is adequate. A moving average of the last $n = 12$ speed measurements is finally introduced as follows

$$\upsilon^{c}_{i,j}(k) = \sum_{l=0}^{n-1} \frac{v^{c}_{i,j}(k-l)}{n}, \tag{16}$$

to calculate the final cell speed $v_{i,j}^{c}(k)$ fed into the Kalman Filter.

Lateral flows of connected vehicles $L_{i,j_1\to j_2}^{c}$ are computed based on position reports of connected vehicles. Specifically, we count first the number of connected vehicles moved from lane j_1 to lane j_2 within a time interval of 2 s; then, every time instant kT, these lateral flow measurements are accumulated for the time interval $((k-1)T,kT]$ to produce an intermediate lane-changing measurement $\overline{L}_{i,j_1\to j_2}^{c}(k)$. This lateral flow vector of connected vehicles, $\overline{L}^{c}$, may exhibit spiky behavior, due to the rare appearance of connected vehicle lateral movements; and therefore, this value may not be representative for the occurring lane-changing flow of the total vehicle population. To account for this fact and obtain representative, though averaged lateral flows, we feed the estimation scheme with an exponentially smoothed version of the lateral flows of connected vehicles, rather than the original measured lateral flows. Thus, for each lateral flow measurement, we have for all $i = 1,...,N, j_1 = 1,...,M$, and $j_2 = j_1 \pm 1$

$$L_{i,j_1\to j_2}^{c}(k+1) = (1-a)L_{i,j_1\to j_2}^{c}(k) + a\overline{L}_{i,j_1\to j_2}^{c}(k), s \tag{17}$$

where the smoothing factor $a \in [0,1]$ is chosen based on statistical analysis (see Section 4.5.2) and $L_{i,j_1\to j_2}^{c}(0) = 0$.

Also for the density measurements $\rho_{i,j}^{c}(k)$, that are fed to the Kalman Filter every time step k, we employ, for similar reasons as above, a moving average of the $m = 6$ (time window of 1 min) latest available measurements as

$$\rho_{i,j}^{c}(k) = \sum_{l=0}^{m-1} \frac{\widetilde{\rho}_{i,j}^{c}(k-l)}{m}, \tag{18}$$

where $\widetilde{\rho}_{i,j}^{c}(k)$ is the instant density at cell (i,j) for every time step k. In cases where there are no connected vehicle reports available at cell (i,j) at a time instant kT, we replace the corresponding $\widetilde{\rho}_{i,j}^{c}(k)$ with the density reported at the previous time step, i.e., we set $\widetilde{\rho}_{i,j}^{c}(k) = \widetilde{\rho}_{i,j}^{c}(k-1)$.

Assuming that the (smoothed) lateral flow of connected vehicles exiting from the lane-drop cell, namely, $L_{8,1\to 2}^{c}$, is always non-zero, it can be shown that the utilized flow measurement configuration, shown in Fig. 2, guarantees observability of the underlying model (8), (9), see Bekiaris-Liberis et al. (2017) for details. Specifically, sets of detectors (one in each lane) located at the highway entrance (0 km) and exit (9.33 km) are used to obtain the input and output of system (8), (9), respectively. All ramp flows are assumed unmeasured; therefore, to establish observability, an additional flow measurement on the right-most lane of a (arbitrarily chosen) segment between every pair of consecutive unmeasured ramps is needed. In the present evaluation, we exceed these minimum measurement requirements for observability by assuming the presence of fixed flow detectors at all lanes (cross-section), rather than only the right-most lane, of the aforementioned segments; this is deemed reasonable, since detectors are usually installed for a cross-section. In conclusion, we employ a set of additional flow detectors (one per lane) located at 3.83 km (segment $i = 9$), 4.52 km (segment $i = 11$), and 6.82 km (segment $i = 15$).

4. Performance evaluation for varying penetration rates of connected vehicles

Based on the microscopic environment configuration described in Section 3, we simulate traffic conditions featuring various penetration rates of connected vehicles. To account for a variety of possible current and future traffic scenarios, the performance of the estimation scheme is evaluated for a wide range of penetration rates of connected vehicles, more specifically, for 2%, 5%, 10%, 20%, and 50%.

4.1. Selection of the estimation scheme parameters

The sensitivity of the estimation performance to the Kalman filter parameters (Q,R) is thoroughly examined in Bekiaris-Liberis et al. (2016), Roncoli et al. (2016a), and Fountoulakis et al. (2017), for the aggregated-lane approach, where it is demonstrated that density estimation is barely sensitive to these parameters, whereas ramp flow estimation is moderately sensitive. Additionally, it has been observed that the choice of the initial values μ and H affects only the warm-up phase of the estimation. Table 1 summarizes the filter parameters used in our experiments, which were chosen based on a sensitivity analysis (see Papadopoulou, 2017).

It should be noted that, since we expect strong diagonal flows mainly at the lane-drop cell (in comparison with the rest of the cells), we set all percentages $p_{i,j_1\to j_2}$, $\overline{p}_{i,j}$ equal to zero except for the percentage

$$p \equiv p_{8,1\to 2}, \tag{19}$$

which corresponds to the diagonal lateral flow of cell (8,2).

Table 1
Filter parameters used in the simulation investigation. The total number of on-ramps and off-ramps are indicated with l_r and l_s, respectively.

Q	σ_ρ	$\sigma_{r,s}$
$\mathrm{diag}(\sigma_\rho,\sigma_{r,s})$	$10 \times I_{(N\times M)}$	$0.01 \times I_{(l_r+l_s)}$
R	μ	H
$10^4 \times I_{(l_r+l_s)}$	$(5,...,5,2,...,2)^T$	$I_{(N\times M+l_r+l_s)}$

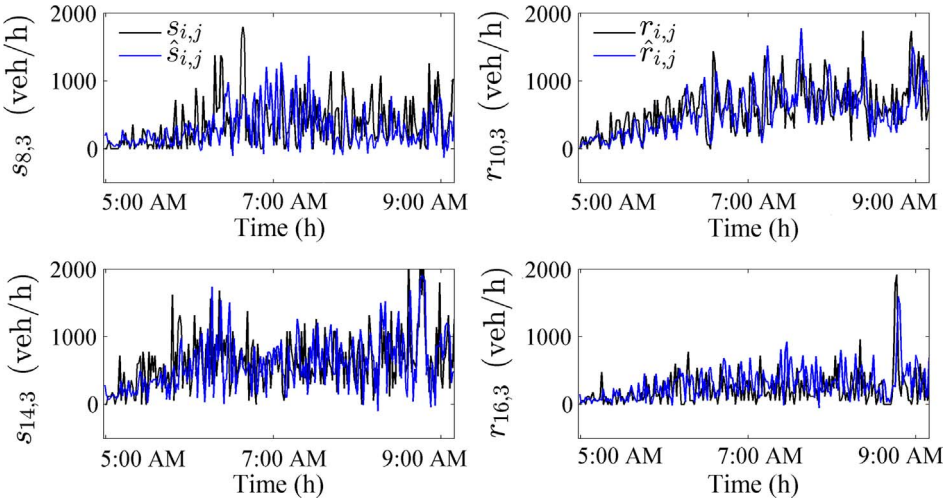

Fig. 4. Comparison between ground truth (black line) and estimated (blue line) ramp flows for all on-ramps and off-ramps in the network. (For interpretation of the references to color in this figure legend, the reader is referred to the web version of this article.)

4.2. Quantitative performance measure

To assess the overall performance of the suggested estimation scheme, a performance index formulated as the Coefficient of Variation (CV) of the root mean square error of the 60-s moving averages of estimated densities $\hat{\rho}_{i,j}$ and ramp flows $\hat{\theta}_i$ with respect to the corresponding ground truth, is adopted as

$$CV_\rho = \frac{\sqrt{\frac{1}{MNK}\sum_{i=1}^{N}\sum_{j=1}^{M}\sum_{k=1}^{K}[\hat{\rho}_{i,j}(k)-\rho_{i,j}(k)]^2}}{\frac{1}{MNK}\sum_{i=1}^{N}\sum_{j=1}^{M}\sum_{k=1}^{K}\rho_{i,j}(k)} \tag{20}$$

$$CV_{r,s} = \frac{\sqrt{\frac{1}{K(l_r+l_s)}\sum_{k=1}^{K}\sum_{i=1}^{l_r+l_s}[\hat{\theta}_i(k)-\theta_i(k)]^2}}{\frac{1}{K(l_r+l_s)}\sum_{k=1}^{K}\sum_{i=1}^{l_r+l_s}\theta_i(k)}, \tag{21}$$

where $\theta_1 = r_{10}$, $\theta_2 = r_{16}$, $\theta_3 = s_{18}$, $\theta_4 = s_{14}$, and $M = 3$, $N = 21$, $l_r = l_s = 2$, $K = 1440$.

4.3. Performance evaluation for a baseline case

For the sake of brevity, only specific results of the cell densities and ramp flow estimation for 20% penetration rate of connected vehicles are presented, as illustrated in Figs. 3 and 4, respectively. The results are obtained with $p = 0.3$ and $a = 0.05$, chosen after a sensitivity analysis (see Section 4.5).

It is evident from the plots that the proposed scheme successfully estimates and tracks the dynamics of both segment densities and ramp flows under various traffic conditions, including congestion and free-flow, as well as for (short-lived) time intervals where no information from connected vehicle reports is available. Density estimation is characterized by a performance index $CV_\rho = 34.4\%$, whereas ramp flow estimation is characterized by a performance index $CV_{r,s} = 78.0\%$.

4.4. Performance evaluation for various penetration rates

Fig. 5 illustrates the performance for density and ramp flow estimation with regard to different penetration rates of connected vehicles. A moderate sensitivity is observed in the performance of the estimation scheme, which is seen to deteriorate with decreasing penetration rates of connected vehicles present at the highway. This is mainly due to the accordingly reduced adequacy of the available traffic information feeding the estimation scheme. In fact, the proportion of time intervals without any connected vehicle in a cell increases with decreasing penetration rate, reaching up to 70% for a penetration rate of 2% (see also Papadopoulou, 2017).

4.5. Sensitivity of the estimation performance to the model parameters

In order to evaluate the sensitivity of the estimation performance to the variations of the model parameters p and a, we perform a series of experiments considering different possible combinations of $p \in [0,1]$ and $a \in [0,1]$, for our basic scenario of 20% penetration rate of connected vehicles.

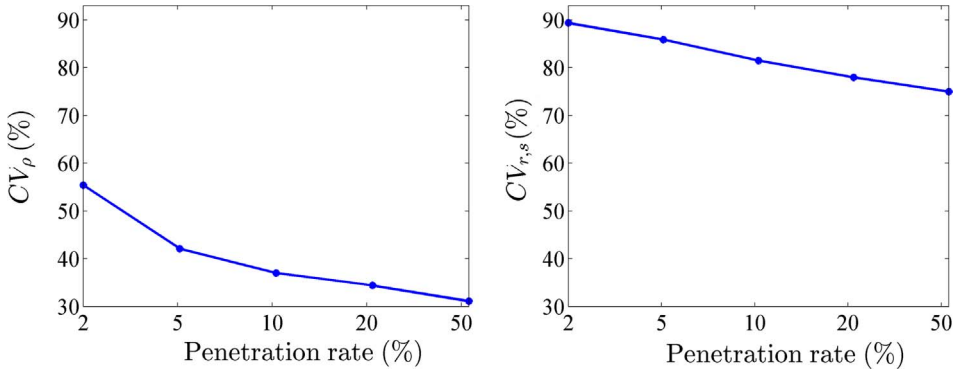

Fig. 5. Performance comparison of density (left) and ramp flow (right) estimations for various penetration rates of connected vehicles.

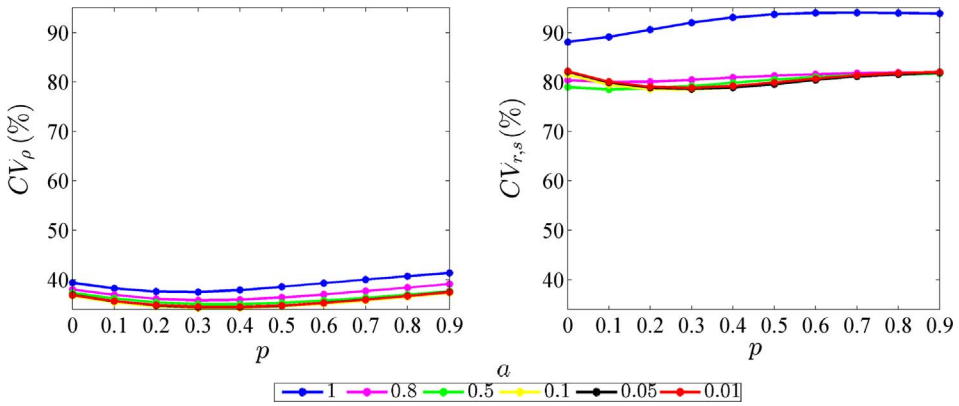

Fig. 6. Performance comparison of the density (left) and ramp flow (right) estimations for different values of the parameters p and a for 20% penetration rate.

From Fig. 6, one can observe that the most accurate density estimation is achieved for a value for $p = 0.3$, irrespectively of the values of a; similarly, for ramp flow estimation, as long as there is sufficient smoothing effect. Good estimates are produced with $a < 0.5$. Since for a value of $a \approx 0.05$ we get the minimal CV_ρ and $CV_{r,s}$ in our experiments (although the differences for values of a smaller than about 0.5 are minor), and this fact was confirmed by further simulations with other penetration rates, we choose the default values of the model parameters to be $p = 0.3$ and $a = 0.05$.

Next, we keep one of the two parameters constant in order to examine the sensitivity of the estimation performance to the variations of the other for different penetrations rates.

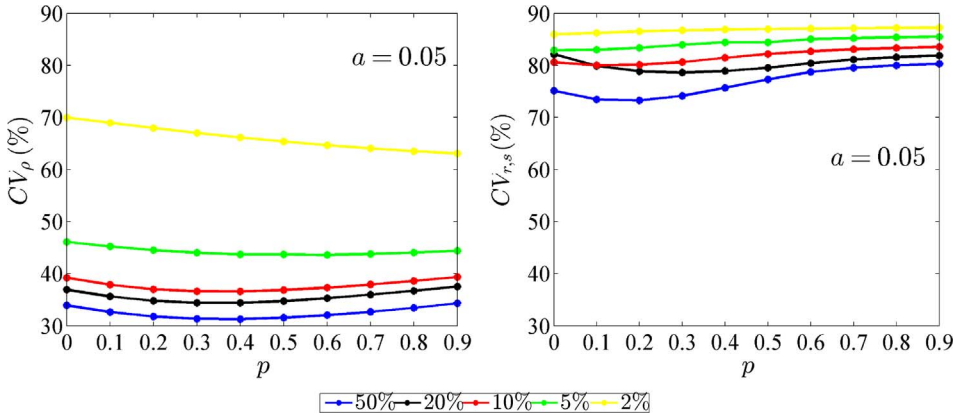

Fig. 7. Performance comparison of the density (left) and ramp flow (right) estimations for different values of the parameter p and for various penetration rates of connected vehicles.

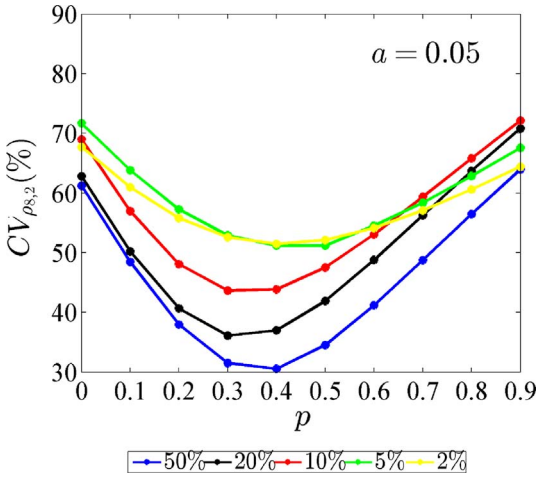

Fig. 8. Performance comparison of density of cell (8,2), adjacent to the lane-drop location, for different values of the parameter p and for various penetration rates of connected vehicles.

4.5.1. Sensitivity analysis for the percentage of lane-drop diagonal flow

We performed experimental analysis to obtain the optimal value of parameter p, prior to be employed in (4), so as to achieve an overall estimation improvement under various penetration rates. Fig. 7 shows the comparison of the performance of the estimation scheme for different values of parameter $p \in [0,1]$, for various penetration rates, while Fig. 8 illustrates the impact of various values of p on the performance index that corresponds specifically to cell (8,2), again for various penetration rates of connected vehicles. During these experiments, we set $a = 0.05$. From Fig. 7 it is evident that, for any given penetration rate, the overall estimation performance is quite insensitive to the different values of parameter p, whereas ramp flow estimation is slightly more sensitive. Density estimation at cell (8,2), is more sensitive to changes of parameter p, as shown in Fig. 8. With regard to the density estimation, a value $p = 0.3$ may well depict the diagonal flows in the model of longitudinal flows (2) for almost all penetration rates, though for very low penetration rates the optimal value shifts towards to $p = 0.5$.

4.5.2. Sensitivity analysis for the smoothing factor

Sensitivity of the estimation performance to the variations of the smoothing factor a is shown in Fig. 9, for $p = 0.3$ and for various penetration rates of connected vehicles. From Fig. 9, one can observe that: (i) the quality of estimates features low sensitivity with regard to a at higher penetration rates; while (ii) at low penetration rates, the density estimation is sensitive to different values of smoothing factor a. This is consistent with the expectation that at lower penetration rates a stronger smoothing effect is beneficial, since the density and lateral flow information from connected vehicles are less accurate. In conclusion, a value of a, which leads to good performance, for all penetration rates, is about 0.05.

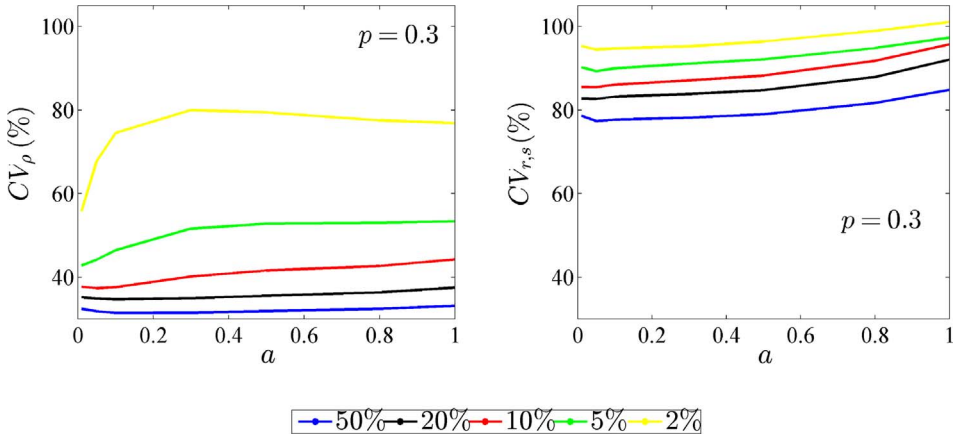

Fig. 9. Performance comparison of density (left) and ramp flow (right) estimations for different values of the smoothing factor a and for various penetration rates of connected vehicles.

5. Conclusions

The validity of a per-lane traffic density and ramp flow estimation scheme, which is based on an appropriate multi-lane traffic flow model and a standard Kalman filter, has been thoroughly tested using the microscopic traffic simulator AIMSUN. The proposed scheme is mainly based on speed and position information obtained from connected vehicle reports. The effectiveness of the proposed methodology was examined in carefully designed experiments for a real highway stretch and real demand scenarios. The obtained results demonstrate that the estimation scheme captures the onset of congestion with accurate timing and more generally, reproduces reliably the challenging traffic conditions in space and time, even for low penetration rates. Density estimation is satisfactory even for penetration rates as low as 2%. An analysis of the sensitivity of the estimation scheme to the model parameters was also presented. In general, the scheme was shown to be little sensitive to the model parameters. The presented approach has several advantages for possible future real-world applications, including:

- the use of a macroscopic model that has now calibration requirements (e.g. no fundamental diagram);
- the extensive use of low-cost connected vehicle data that are already available and are expected to increase in the near future;
- the use of only a limited amount of fixed flow sensors.

It should be emphasized that the availability of real-time traffic density per lane estimates is a prerequisite for the application of lane-based traffic control algorithms.

Acknowledgment

This research was supported by the European Research Council under the European Union's Seventh Framework Programme (FP/2007-2013)/ERC Advanced Grant Agreement n. 321132, project TRAMAN21.

The authors would like to thank Prof. Bart van Arem and his group for their support in providing information related to the network used in the case study.

References

Anand, A., Ramadurai, G., Vanajakshi, L., 2014. Data fusion-based traffic density estimation and prediction. J. Intell. Transport. Syst. 18 (4), 367–378.
Bekiaris-Liberis, N., Roncoli, C., Papageorgiou, M., 2016. Highway traffic state estimation with mixed connected and conventional vehicles. IEEE Trans. Intell. Transport. Syst. 17 (12), 3484–3497.
Bekiaris-Liberis, N., Roncoli, C., Papageorgiou, M., 2017. Structural observability of multi-lane traffic with connected vehicles. In: IEEE Conference on Intelligent Transportation Systems. Yokohama, Japan.
Carey, M., Balijepalli, C., Watling, D., 2015. Extending the cell transmission model to multiple lanes and lane-changing. Netw. Spat. Econ. 15 (3), 507–535.
Chalko, T.J., 2007. High accuracy speed measurement using GPS (global positioning system). NU J. Discov. 4, 1–9.
Chang, M.-F., Gazis, D.C., 1975. Traffic density estimation with consideration of lane-changing. Transport. Sci. 9 (4), 308–320.
Coifman, B., 2003. Estimating density and lane inflow on a freeway segment. Transport. Res. Part A: Pol. Pract. 37 (8), 689–701.
De Fabritiis, C., Ragona, R., Valenti, G., 2008. Traffic estimation and prediction based on real time floating car data. In: IEEE Conference on Intelligent Transportation Systems, pp. 197–203.
Deng, W., Lei, H., Zhou, X., 2013. Traffic state estimation and uncertainty quantification based on heterogeneous data sources: a three detector approach. Transport. Res. Part B: Methodol. 57, 132–157.
Du, L., Gong, S., Wang, L., Li, X.-Y., 2016. Information-traffic coupled cell transmission model for information spreading dynamics over vehicular ad hoc network on road segments. Transport. Res. Part C: Emerg. Technol. 73, 30–48.
Fountoulakis, M., Bekiaris-Liberis, N., Roncoli, C., Papamichail, I., Papageorgiou, M., 2017. Highway traffic state estimation with mixed connected and conventional vehicles: microscopic simulation-based testing. Transport. Res. Part C: Emerg. Technol. 78, 13–33.
Herrera, J.C., Bayen, A.M., 2010. Incorporation of lagrangian measurements in freeway traffic state estimation. Transport. Res. Part B: Methodol. 44 (4), 460–481.
Herrera, J.C., Work, D.B., Herring, R., Ban, X.J., Jacobson, Q., Bayen, A.M., 2010. Evaluation of traffic data obtained via GPS-enabled mobile phones: the mobile century field experiment. Transport. Res. Part C: Emerg. Technol. 18 (4), 568–583.
Laval, J.A., Daganzo, C.F., 2006. Lane-changing in traffic streams. Transport. Res. Part B: Methodol. 40 (3), 251–264.
Liu, K., Yamamoto, T., Morikawa, T., 2006. An analysis of the cost efficiency of probe vehicle data at different transmission frequencies. Int. J. ITS Res. 4 (1), 21–28.
Papadopoulou, S., 2017. Microscopic simulation-based validation of a per lane traffic state estimation scheme on highways with connected vehicles, Master's thesis. School of Production Engineering and Management, Technical University of Crete.
Papageorgiou, M., Diakaki, C., Nikolos, I., Ntousakis, I., Papamichail, I., Roncoli, C., 2015. Freeway traffic management in presence of vehicle automation and communication systems (VACS). In: Road Vehicle Automation 2. Springer, pp. 205–214.
Papageorgiou, M., Messmer, A., 1999. Metanet: a macroscopic simulation program for motorway networks. Traf. Eng. Control 31 (8-9), 466–470.
Perraki, G., Roncoli, C., Papamichail, I., Papageorgiou, M., 2017. Evaluation of an MPC strategy for motorway traffic comprising connected and automated vehicles. In: IEEE Conference on Intelligent Transportation Systems. Yokohama, Japan.
Piccoli, B., Han, K., Friesz, T.L., Yao, T., Tang, J., 2015. Second-order models and traffic data from mobile sensors. Transport. Res. Part C: Emerg. Technol. 52, 32–56.
Qiu, T., Lu, X.-Y., Chow, A., Shladover, S., 2010. Estimation of freeway traffic density with loop detector and probe vehicle data. Transport. Res. Rec.: J. Transport. Res. Board 2178, 21–29.
Rahmani, M., Koutsopoulos, H.N., Ranganathan, A., 2010. Requirements and potential of GPS-based floating car data for traffic management: Stockholm case study. In: IEEE Conference on Intelligent Transportation Systems, pp. 730–735.
Rempe, F., Franeck, P., Fastenrath, U., Bogenberger, K., 2016. Online freeway traffic estimation with real floating car data. In: IEEE Conference on Intelligent Transportation Systems, pp. 1838–1843.
Roncoli, C., Bekiaris-Liberis, N., Papageorgiou, M., 2016a. Highway traffic state estimation using speed measurements: case studies on NGSIM data and highway A20 in the Netherlands. Transport. Res. Rec.: J. Transport. Res. Board 2559, 90–100.
Roncoli, C., Bekiaris-Liberis, N., Papageorgiou, M., 2016b. Optimal lane-changing control at motorway bottlenecks. In: IEEE Conference on Intelligent Transportation Systems, pp. 1785–1791.
Roncoli, C., Bekiaris-Liberis, N., Papageorgiou, M., 2017. Lane-changing feedback control for efficient lane assignment at motorway bottlenecks. Transport. Res. Rec.: J. Transport. Res. Board 2625, 20–31.
Roncoli, C., Papageorgiou, M., Papamichail, I., 2015. Traffic flow optimisation in presence of vehicle automation and communication systems–part ii: optimal control

for multi-lane motorways. Transport. Res. Part C: Emerg. Technol. 57, 260–275.
Schakel, W.J., Van Arem, B., 2014. Improving traffic flow efficiency by in-car advice on lane, speed, and headway. IEEE Trans. Intell. Transport. Syst. 15 (4), 1597–1606.
Schreiter, T., van Lint, H., Treiber, M., Hoogendoorn, S., 2010. Two fast implementations of the adaptive smoothing method used in highway traffic state estimation. In: IEEE Conference on Intelligent Transportation Systems, pp. 1202–1208.
Seo, T., Bayen, A.M., Kusakabe, T., Asakura, Y., 2017. Traffic state estimation on highway: a comprehensive survey. Ann. Rev. Contr. 43, 128–151.
Seo, T., Kusakabe, T., 2015. Probe vehicle-based traffic state estimation method with spacing information and conservation law. Transport. Res. Part C: Emerg. Technol. 59, 391–403.
Seo, T., Kusakabe, T., Asakura, Y., 2015. Estimation of flow and density using probe vehicles with spacing measurement equipment. Transport. Res. Part C: Emerg. Technol. 53, 134–150.
Singh, K., Li, B., 2012. Discrete choice modelling for traffic densities with lane-change behaviour. Proc.-Soc. Behav. Sci. 43, 367–374.
Transport Simulation Systems, 2014. Aimsun 8 Dynamic Simulators Users' Manual. Transport Simulation Systems.
Treiber, M., Kesting, A., Wilson, R.E., 2011. Reconstructing the traffic state by fusion of heterogeneous data. Comp.-Aided Civil Infrastruct. Eng. 26 (6), 408–419.
Turksma, S., 2000. The various uses of floating car data.
van Hinsbergen, C.P., Schreiter, T., Zuurbier, F.S., Van Lint, J., van Zuylen, H.J., 2012. Localized extended kalman filter for scalable real-time traffic state estimation. IEEE Trans. Intell. Transport. Syst. 13 (1), 385–394.
Wang, R., Work, D.B., Sowers, R., 2016. Multiple model particle filter for traffic estimation and incident detection. IEEE Trans. Intell. Transport. Syst. 17 (12), 3461–3470.
Wang, Y., Papageorgiou, M., 2005. Real-time freeway traffic state estimation based on extended kalman filter: a general approach. Transport. Res. Part B: Methodol. 39 (2), 141–167.
Waterson, B., Box, S., 2012. Quantifying the impact of probe vehicle localisation data errors on signalised junction control. IET Intell. Transp. Syst. 6 (2), 197–203.
Work, D.B., Tossavainen, O.-P., Blandin, S., Bayen, A.M., Iwuchukwu, T., Tracton, K., 2008. An ensemble kalman filtering approach to highway traffic estimation using GPS enabled mobile devices. In: IEEE Conference on Decision and Control, pp. 5062–5068.
Wright, M., Horowitz, R., 2016. Fusing loop and GPS probe measurements to estimate freeway density. IEEE Trans. Intell. Transport. Syst. 17 (12), 3577–3590.
Yılan, M., 2016. Multilane Traffic Density Estimation with KDE and Nonlinear LS and Tracking with Scalar Kalman Filtering. Master's thesis.
Yuan, Y., Van Lint, J., Wilson, R.E., van Wageningen-Kessels, F., Hoogendoorn, S.P., 2012. Real-time lagrangian traffic state estimator for freeways. IEEE Trans. Intell. Transport. Syst. 13 (1), 59–70.
Zhao, X., Carling, K., Håkansson, J., 2014. Reliability of GPS Based Traffic Data: An Experimental Evaluation. Högskolan Dalarna.
Zhou, Z., Mirchandani, P., 2015. A multi-sensor data fusion framework for real-time multi-lane traffic state estimation. In: Transportation Research Board 94th Annual Meeting, Number 15-0186.
Zito, R., D'este, G., Taylor, M., 1995. Global positioning systems in the time domain: how useful a tool for intelligent vehicle-highway systems? Transport. Res. Part C: Emerg. Technol. 3 (4), 193–209.